Co-delivery of siRNAs and Anti-cancer Drugs Using Layered Double Hydroxide Nanoparticles

Li Li[a], Wenyi Gu[a]*, Jiezhong Chen[b,c], Weiyu Chen[a], Zhi Ping Xu[a]*

[a] *Australian Institute for Bioengineering and Nanotechnology, The University of Queensland, Brisbane, QLD 4072, Australia*

[b] *School of Biomedical Sciences, University of Queensland, St Lucia, QLD 4072*

[c] *Faculty of Science, Medicine and Health, University of Wollongong, Northfields Avenue, NSW 2522, Australia.*

Fax: 61 7 33463973; Tel: 617 33463809; E-mail: gordonxu@uq.edu.au; w.gu@uq.edu.au

Keywords: Co-delivery system, Layered double hydroxide, Electrostatic assembly, Apoptosis.

Abstract:

In this research we employed layered double hydroxide nanoparticles (LDHs) to simultaneously deliver an anticancer drug 5-fluorouracil (5-FU) and Allstars Cell Death siRNA (CD-siRNA) for effective cancer treatment. The strategy takes advantage of the LDH anion exchange capacity to intercalate 5-FU into its interlayer spacing and load siRNA on the surface of LDH nanoparticles. LDH nanoparticles have been demonstrated as an effective cellular delivery system for 5-FU and siRNA separately in this and other investigations. More excitedly, the combination of CD-siRNA and anticancer drug 5-FU with the same LDH particles significantly enhanced cytotoxicity to three cancer cell lines, e.g. MCF-7, U2OS and HCT-116, compared to the single treatment with either CD-siRNA or 5-FU. This result is probably a result of coordinate mitochondrial damage process. Thus, the strategy to co-deliver siRNA and an anticancer drug by LDHs has great potential to overcome the drug resistance and enhance cancer treatment.

1. Introduction

Chemotherapy is one of most common cancer treatments in clinics. In most cases, the clinical responses show that the efficacy of chemotherapy is limited by the development of multidrug resistance (MDR) in cancer cells during a long period of treatment [1, 2]. To overcome the resistance, higher doses of toxic anticancer drugs are sometimes required, which can also kill healthy cells and result in adverse side effects on healthy organs [3]. Thus, the development of an effective strategy to overcome the multidrug resistance in chemotherapy remains a major challenge in the treatment of cancers.

One strategy is to combine two different types of anticancer therapeutics for effective cancer treatment [6-8], for example, co-deliver 5-fluorouracil (5-FU) and small interfering RNAs (siRNAs). 5-FU has been used against cancers for over 40 years and acts principally as a thymidylate synthase inhibitor [4]. Drug resistance is a major issue in the clinical application of 5-FU. siRNA molecules, in contrast, have emerged as a powerful tool to suppress tumor growth due to their properties to induce potent, persistent, and specific silencing of a broad range of genetic targets [5, 6]. Therefore, a combination of the anticancer drug 5-FU and siRNA for advanced cancer treatment could be an effective way to overcome MDR [7-9]. In recent years, several groups have reported significant improvements using combined cancer therapies. For example, Nakamura et al. reported that the combination of siRNA against Bcl-2 and 5-FU delivered by lipoplexes showed superior tumor inhibition compared to the monotherapy with either 5-FU or Bcl-2-siRNA [10]. More recently, Chen et al. found that mesoporous silica nanoparticles can been used to co-deliver doxorubicin with siRNA against Bcl-2 or p-

This is a post-print version of the following article: Li, Li, Gu, Wenyi, Chen, Jiezhong, Chen, Weiyu and Xu, Zhi P. (2014) Co-delivery of siRNAs and anti-cancer drugs using layered double hydroxide nanoparticles. *Biomaterials*, *35* 10: 3331-3339.

glycoprotein, resulting in significantly increased cytotoxic effects on multidrug resistant cancer cells *in vitro* [11].

Although the combination of chemotherapy and siRNA-based therapy for advanced cancer treatment has shown great promise, an ideal delivery system that can elegantly accommodate siRNAs and chemotherapeutic drugs and effectively co-deliver them to cancer cells would further enhance cancer treatment efficacy. Currently, liposomes and cationic core-shell nanoparticles [3, 12, 13] have been used to simultaneously deliver drugs and siRNAs into cancer cells, while the drug-siRNA-carrier system can be rationally designed to further improve anti-cancer efficiency. It is our belief that layered double hydroxide (LDH) nanoparticles are one of the more effective carrier and delivery systems.

Layered double hydroxides (LDHs), a family of anionic clay materials, are considered promising inorganic matrices for drug and gene delivery due to their unique properties, such as high layer charge density (2-5 mequiv/g), anion exchange property, low cytotoxicity, pH-controlled release, good biocompatibility, tunable particle size, and protection of drugs and genes during the delivery process [14, 15]. LDHs consist of cationic brucite-like layers and interlayer anions with the general chemical composition $M^{2+}_{1-x}M^{3+}_{x}(OH)_2\ (A^{n-}_{x/n})\cdot yH_2O$, where M^{2+} and M^{3+} are divalent and typically trivalent metal cations respectively, A^{n-} an anion, and x the molar ratio of the trivalent to the total cations [16]. The anionic drugs and biomolecules (including genetic materials) can be easily exchanged with the interlayer anion A^{n-}, and are thus protected against enzymatic degradation. Recent studies have demonstrated that LDHs are an efficient carrier to deliver anionic anticancer drugs such as methotrexate (MTX) [17, 18] and 5-FU [19, 20], and functional oligonucleotides, especially siRNAs [21, 22], for cancer treatment. Choy *et al*

reported that MTX delivered by LDHs significantly enhanced drug efficacy compared to free MTX in human osteosarcoma cells (HOS, SaOS-2 and MG-63) [23, 24]. In our previous studies, LDH-mediated siRNAs effectively silenced the target gene expressions [21, 22, 25]. It is clear that the single treatment by either anticancer drug or siRNA delivered by LDH nanoparticles can only achieve limited success in cancer treatment, while the co-delivery of anticancer drugs and siRNA that are elegantly combined with LDH nanoparticles would synergistically enhance the efficacy in cancer treatment. To our knowledge, there are no reports on simultaneously delivering a traditional anticancer drug and siRNA to cancer cells using LDH nanocarriers for enhanced cancer therapy.

As illustrated in Scheme 1A, LDH nanocarriers first intercalate with 5-FU into the interlayers to form 5-FU/LDH nanohybrids, and then load CD-siRNA to form CD-siRNA-5-FU/LDH nanocomplexes via the electrostatic interactions between negatively charged siRNAs and positively charged 5-FU/LDH. In this work, we aimed to investigate whether 5-FU and CD-siRNA can be efficiently co-delivered into the cancer cells by LDH nanocarriers and to what extent the combined treatment with 5-FU and CD-siRNA may enhance the suppression of cell growth compared to single treatment with either CD-siRNA/LDH or 5-FU/LDH alone.

2. Materials and Methods

2.1 Materials

$MgCl_2 \cdot 6H_2O$, $AlCl_3 \cdot 6H_2O$, NaOH, 5-FU, bovine serum albumin, Tween 20, and lysis buffer were purchased from Sigma (USA). AllStars Cell Death siRNA (CD-siRNA) and AllStars negative controlled fluorescent siRNA AF 546 (CD-siRNA AF546) were purchased from

QIAGEN Pty. Ltd. (Vic, Australia). GelRed Nucleic acid gel stain was bought from Biotium Inc. (USA). Agarose, 25-bp dsDNA ladder mark, 0.25% Trypsin-EDTA (1X), PBS buffer (37mmol/L NaCl, 2.7 mmol/L KCl, 8.1 mmol/L Na_2HPO_4, and 1.47 mmol/L KH_2PO_4, pH 7.4), Tris-buffer and DMEM medium were obtained from Life Technologies Corporation (Australia). BD Pharmingen™ FITC Annexin V Apoptosis Detection Kit I was obtained from BD Biosciences (USA). A Bio-Rad DC Protein Assay kit was purchased from Bio-Rad Laboratories (CA). Mouse monoclonal anti-human Bcl-2 antibody and mouse monoclonal anti-human α-tubulin antibody were bought from Bio-legend (CA).

2.2 Preparation of 5-FU/LDH nanohybrids

Mg_2Al-LDH-Cl nanoparticles (LDH-Cl) were prepared using the co-precipitation-hydrothermal method reported previously [26], and 5-FU/Mg_2Al-LDH-Cl (5-FU/LDH) nanohybrids were synthesized similarly. In brief, a mixture of 0.3 M $MgCl_2$ and 0.1 M $AlCl_3$ solution (10 mL) was quickly added to 40 mL of 0.15 M NaOH solution under vigorous stirring. After stirring for 10 min, the LDH slurry was collected via centrifuge separation and re-suspended in 40 mL of solution containing a certain amount of 5-FU (neutralized with dilute NaOH solution, with pH of 8-9) and shaken for 1 h at 37^{o}C. The resultant suspension was separated, washed and then re-suspended in 40 mL distilled water. The inhomogeneous suspension was transferred to an autoclave (stainless steel with a Teflon lining) and heated in an oven at 100 ^{o}C for 16 h. After hydrothermal treatment, a transparent, homogenous suspension containing 5-FU/LDH was obtained. The loading amount of 5-FU drug was determined using UV-Vis. The samples were marked as 5-FU(n)/LDH, where n equals the exchange capacity of 5-FU in LDH-Cl samples.

2.3 Preparation of siRNA or dsDNA-5-FU/LDH nanohybrids

A predetermined amount of dsDNA was added to a vial containing an appropriate amount of 5-FU/LDH or LDH to make the dsDNA-5-FU/LDH or dsDNA/LDH with the mass ratio of dsDNA to LDH equal to 1:5, 1:10, 1:20 and 1:40, respectively. The mixture suspension was shaken via a vortex for 15 s and then kept still at room temperature for 1 h. CD-siRNA/LDH and CD-siRNA-5-FU/LDH nanohybrids were prepared in the same way with the mass ratio of CD-siRNA to LDH approximately 1:20 and 1:40, respectively.

2.4 Physicochemical characterization

The hydrodynamic particle size and the zeta potential of LDH and 5-FU/LDH nanohybrids were determined by dynamic light scattering (DLS). All measurements were carried out at 25 ^{o}C in a photon correlation spectroscopy (PCS, Nanosizer Nano ZS, MALVERN Instruments). Each parameter was measured in triplicate and the average value was calculated. Powder X-ray diffraction (XRD) patterns were recorded on a Rigaku Miniflex X-ray diffractometer with a variable slit width at a scanning rate of 2°/min with 2θ ranging from 2.5° to 80° using Co Kα radiation (λ=0.17902 nm). The LDH or 5-FU/LDH suspension was placed onto a quartz sample holder with the zero background and then air-dried to form a thin film for XRD pattern collection. Transmission electron microscopy (TEM) images were obtained on a JEOL 1010A transmission electron microscope at an acceleration voltage of 100 kV. The loading amount of 5-FU into LDH were determined by UV-Vis absorbance at 265 nm. Mg and Al contents in all samples were determined by inductive coupled plasma - atomic emission spectroscopy (ICP-AES) on a Varian

Vista Pro instrument. Element analysis of C, H and N was conducted using Flash EA 1112 CHNS-O analyser (Thermo Electron Corp., US)

2.5 Agarose gel electrophoresis

The binding ability of CD-siRNA with 5-FU/LDH or LDH nanoparticles was evaluated by gel retardation. In this test, the mimic dsDNA was used instead of CD-siRNA. In typical gel retardation, 20 μL of dsDNA-5-FU/LDH nanocomplexes containing 200 ng of dsDNA was loaded into the well in a 2% agarose gel containing GelRed stain, followed by electrophoresis at 80 V for 40 min. The gel was analyzed on a GelDoc UV illuminator (Biorad Laboratories) to show the position of the dsDNA band relative to that of free dsDNA.

2.6 Cell culture and cellular uptake

Human breast (MCF-7), osteosarcoma (U2OS) and colorectal (HCT-116) cancer cell lines were routinely cultured in a DMEM medium supplemented with 10% fetal calf serum and penicillin (10 U/mL)/streptomycin (10 μg/mL) in a humidified atmosphere at 37 ^{o}C under 5% CO_2. For cellular uptake, MCF-7 cells were seeded on the coverslips in a 6-well plate at a density of 1×10^6 cells cm^{-2} and cultured for 24 h. Neg-siRNA AF546 was used to evaluate the cellular uptake of siRNA-5-FU/LDH nanocomplexes. After incubating for 24 h, 1 mL of red-free medium containing Neg-siRNA AF546-5-FU/LDH nanocomplexes was added into the plate and the cells were incubated for 4 h. Then, cells were washed twice with a PBS buffer, fixed and moved to the glass slides containing a DAPI mounting medium. After nucleus staining, the confocal images were taken on Carl Zeiss LSM 710 confocal laser scanning microscope AFM CLSM.

2.7 Cell viability test

Cell viability was determined by the 3-(4, 5-dimethylthiazol-2-yl)-2,5-diphenyltetrazolium bromide (MTT) assay. In all experiments, cancer cells (MCF-7, U2OS and HCT116) were seeded in 24-well plates at a density of 5×10^4 cells per well in 500 μL of culture medium and incubated for 24 h to allow cell attachment. Following the attachment, the cells were incubated in a fresh medium (500 μL/well) containing 5-FU, 5-FU/LDH, CD-siRNA-5-FU/LDH or CD-siRNA/LDH at the 5-FU concentration ranging from 0.6 to 9.6 μg/mL and the siRNA concentration of 40 nM for 72 h. Then, 50 μL of 5 mg/ml MTT was added to each well. After incubating for 4 h in a dark room, the MTT containing medium was removed and 250 μL of DMSO was added to each well to dissolve the MTT formazan. Absorbance of converted dye was measured at 570 nm with a background subtraction at 650 nm using an ELISA plate reader (Bio-Tek, USA). Cell viability was calculated using the following equation:

$$\text{Cell viability } (\%) = (A_s / A_{control}) \times 100$$

where A_s was the absorbance of cells treated under various conditions and $A_{control}$ was the absorbance of the cells in the standard medium.

2.8 Apoptosis

A FITC Annexin V Apoptosis Detection Kit I was used to identify the early apoptotic cells. MCF-7 cells were seeded in a 6-well plate at a density of 1×10^6 cells/well. After incubating for 24 h, 1 mL of fresh medium containing 5-FU, LDH, 5-FU/LDH, CD-siRNA/LDH, CD-siRNA-5-FU/LDH, or negative siRNA-5-FU/LDH was added to each well. After incubating for 24 h, the

cells were collected and stained with Annexin V conjugated FITC and PI according to the manufacturer's instructions. The apoptotic and necrotic cells in the cell population were analyzed using the software Flow Jo.

2.9 Western blotting

MCF-7 cells were seeded in a 6-well plate at a density of 1×10^6 cells/well. After incubating for 24 h, 1 mL of fresh medium containing 5-FU, LDH, 5-FU/LDH, CD-siRNA/LDH, CD-siRNA-5-FU/LDH, or negative siRNA-5-FU/LDH was added to each well. After transfection for 24 h, the cells were collected for the western blotting test as described below.

Treated cells were washed with chilled PBS buffer and lysed in ice-cold lysis buffer. The lysate samples were centrifuged at 4^0C for 10 mins at 15000g. The protein concentrations in lysates were determined with Bio-Rad DC Protein Assay kit according to the manufacturer's recommended instructions. Equivalent amounts of protein (40 μg) from each cell lysate were separated on a pre-casting gel and transferred electrophoretically onto Hybond-ECL. The membranes were blocked with Tris-buffered saline containing 0.05% Tween 20 and 3% nonfat dry milk powder for 1 hour at room temperature and then incubated overnight at 4 ℃ with primary antibodies: mouse monoclonal anti-human Bcl-2 antibody and mouse monoclonal anti-human α-tubulin antibody, respectively. α-tubulin was used as a loading control. Following three washes with Tris-buffered saline containing 0.05% Tween 20, membranes were incubated with horseradish peroxidase-conjugated goat anti-mouse secondary antibody (MP Biomedicals, Solon, OH) for 1 hour at room temperature. After an additional three washes with Tris-buffered saline

containing 0.05% Tween 20, membranes were analyzed on a GelDoc UV illuminator (Biorad Laboratories).

2.10 Statistical analyses

Data are presented as mean ± SEM and analyzed by one-way ANOVA with Bonferroni post-tests using GraphPad Prism software; a p-value < 0.05 was considered statistically significant.

3. Results and discussion

3.1 Characteristics of 5-FU/LDH nanohybrids

In our previous studies, homogeneous LDH-Cl nanoparticle suspension with the size of approximately 100 nm was prepared using the co-precipitation and hydrothermal treatment method [16]. Based on this method, we loaded 5-FU into LDH nanoparticles via the ion-exchange process. Stable 5-FU/LDH nanohybrid suspension was obtained and the structural characteristics of 5-FU/LDH nanohybrids were examined. As shown in Fig. 1A, the XRD patterns of pristine LDH-Cl particles presented strong and symmetric (00*l*) reflections, corresponding to (003) and (006) and demonstrating the formation of crystalline layered compounds. The basal spacing of LDH-Cl was 0.76 nm, identical to the value reported in the literature [16]. In comparison, the (00*l*) reflections of 5-FU(10)/LDH nanohybrids became weaker and broader, suggesting the reduced crystallinity of the LDH phase. It appears that the (003) peak in 5-FU(50)/LDH nanohybrids was composed of two overlapping peaks at 12.3^{o} and 14.3^{o}, respectively. The low-angle peak (12.3^{o}) could be induced by the intercalation of 5-FU into LDH layers and the basal spacing of 5-FU(50)/LDH layered phase was determined to be

0.83 nm. As the thickness of the LDH-Cl layer is ~0.48 nm, the gallery height corresponding to the (003) peaks in 5-FU(50)/LDH is thus 0.35 nm, very close to the thickness of 5-FU (0.34 nm) [27], suggesting that 5-FU molecules are horizontally, not vertically, intercalated into the LDH interlayers [28], as shown in Scheme 1B. The horizontal intercalation of 5-FU into LDH is different from the observation by Xu et al. They observed that 5-FU was vertically intercalated into the LDH interlayer, where they used ammonia as the base to co-precipitate 5-FU with LDH [29].

As shown in Fig. 1B, 5-FU/LDH nanohybrids had a narrow particle size distribution in the range of 50-150 nm. Compared with LDH-Cl, the average size of 5-FU/LDH decreased from 109 nm to 85 nm, as listed in Table 1. This is probably due to the inhibition of the hydroxide layer growth along the *a* and *b* axes by the anionic organic drug 5-FU, as proposed in the previous study [30]. The zeta potential was around +40.6 mV, close to that of LDH-Cl nanoparticles (+42.2 mV). The similarity in zeta potential probably indicates that 5-FU loading by means of ion exchange results in the similar surface charge and the similar dispersion state, suggesting a similar affinity of ionized 5-FU and Cl^- for LDHs.

As imaged in Fig. 1C, 5-FU(10)/LDH nanohybrids were plate-like particles of an almost hexagonal shape, similar to that of LDH-Cl [16]. The lateral dimension of 5-FU(10)/LDH in Fig. 1C was found in the range of 50-150 nm, in good agreement with the DLS data in Fig. 1B.

FT-IR spectra of 5-FU/LDH, LDH and pure sodium-5-FU (Na-5FU) samples are shown in Fig. 1D. The spectrum of LDH had strong bands at 767, 667 and 549 cm^{-1}, corresponding to M–O vibrations and M–O–H bending [26]. An additional peak at 1365 cm^{-1} was seen from LDH-Cl, resulting from some CO_3^{2-} contamination [31]. As expected, these characteristic peaks of the

LDH phase also appeared in 5-FU(50)/LDH sample, suggesting its nature of LDH material. Since 5-FU exists in an ionic form in the LDH layer (Scheme 1B), we prepared Na-5FU samples by neutralizing with NaOH to pH 9 for the comparison in FT-IR spectra. Notably, two strong peaks at 1650 and 1540 cm^{-1}, characteristic bands of Na-5FU, were tentatively assigned to the stretching vibrations of C=O and C=N bonds [32], which were clearly observed in 5-FU(50)/LDH nanohybrids at 1675 and 1545 cm^{-1} (Fig. 1D). Moreover, the bands at 1220 cm^{-1}, attributing to C-F stretching band for Na-5FU, was also shown in 5-FU(50)/LDH nanohybrids. This suggests that ionized 5-FU was successfully intercalated in the LDH interlayer.

Element analysis confirms 5-FU loading into LDH and reveals the composition of as-obtained samples. As listed in Table 1, the loading amount of 5-FU in 5-FU(10)/LDH and 5-FU(50)/LDH was found 5.12 and 22.60 wt%, respectively. The Mg/Al atomic ratio from ICP measurement was 1.9~2.1, close to the nominal ratio (2.0). Based on these data, the chemical composition of LDHs, 5-FU(10)/LDH, and 5-FU(50)/LDH nanohybrids was approximately $Mg_{1.9}Al(OH)_{5.8}(CO_3^{2-})_{0.05}Cl_{0.9}\cdot 1.5H_2O$, $Mg_{2.1}Al(OH)_{6.2}(5\text{-}FU)_{0.1}(1/2CO_3^{2-},Cl)_{0.9}\cdot 1.5H_2O$ and $Mg_{2.1}Al(OH)_{6.2}(5\text{-}FU)_{0.5}(1/2CO_3^{2-},Cl)_{0.5}\cdot 1.5H_2O$, respectively. In the following studies, 5-FU(10)/LDH sample was used for cell tests as its loading amount of 5-FU was sufficiently high.

3.2 Binding capacity of siRNA for 5-FU/LDH nanohybrids

To investigate whether and to what extent the 5-FU loading in the LDH layer has effect on siRNA-LDH interaction, the siRNA binding ability of 5-FU/LDH was investigated through the agarose gel retardation assay. Due to siRNA's intrinsic instability and high cost, mimic dsDNA with the same size and sequence was used in the experiment. As shown in Fig. 2, free dsDNA

migrated to the bottom and exhibited a bright band. Clearly, no bright dsDNA bands were observed at the bottom when the mass ratio of 5-FU/LDH to dsDNA was more than 10:1. Instead, the majority of the dsDNA remained in the loading well and a very small portion of associated dsDNA was dissociated and slowly migrated toward the bottom during electrophoresis, indicating retardation of DNA mobility due to neutralization of the dsDNA negative charge by the surface positive charge of 5-FU/LDH nanohybrids. When the mass ratio of 5-FU/LDH to dsDNA decreased to 5:1, a weak band was observed at the bottom, indicating a small amount of free DNA in the solution. This suggests that 5-FU/LDH nanohybrids can effectively bind with dsDNA at the mass ratio of LDH to dsDNA over 10:1.

Compared to pristine LDH-Cl, 5-FU/LDH nanohybrids presented a similar dsDNA binding efficiency. As shown in Fig. S1, similar phenomena could be observed when LDH-Cl was used to bind the mimic dsDNA. The similarity in binding dsDNA could be explained by the comparable zeta potentials of 5-FU/LDH (+40.6 mV) and LDH-Cl (+42.2 mV), e.g. 5-FU/LDH nanohybrids and LDH-Cl nanoparticles display similar electrostatic interactions with dsDNA or siRNA. This further demonstrates that 5-FU loading has no obvious effect on the binding property of LDH-Cl. Therefore, LDH nanoparticles can simultaneously carry 5-FU and dsDNA/siRNA in a stable colloid at the mass ratio of LDH to dsDNA or siRNA over 10:1.

3.3 Cellular uptake and intercellular localization

The cellular internalization of siRNA and 5-FU into the cells was investigated by complexing LDH-Cl nanoparticles or 5-FU/LDH nanohybrids with red-flourescence negative control siRNA (Red siRNA 456). Cell nuclei were stained with DAPI. As shown in Fig. 3A and 3B, strong red

fluorescence was observed in the perinuclear region in the MCF-7 cytoplasm for both LDH-Cl and 5-FU/LDH with similar red fluorescence intensities (40 nM Red siRNA 546, the mass ratio of siRNA:LDH = 1:40, 4-h incubation). The similar red-fluorescent cells were also observed at the siRNA:LDH mass ratio of 1:20 (Fig. S2A and S2B). In contrast, no red fluorescence was observed in MCF-7 cells after incubating with free Red-siRNA 546 (data not shown here), which is consistent with our previous reports that free siRNA does not efficiently penetrate the plasma membrane [33]. These data clearly show that 5-FU/LDH nanohybrids are able to enter into cancer cells and simultaneously deliver 5-FU and siRNA into the cytoplasm, confirming our hypothesis that LDH can effectively co-deliver the anti-cancer drug and siRNA into the cancer cells.

It is noteworthy that the red puncta shown in Fig. 4B are likely to be early endosomes and multivesicular bodies, which have previously been demonstrated as the internalization route for LDH nanoparticles [22, 25, 31, 34]. Thus, 5-FU/LDH entry into MCF-7 invovles a clathrin-mediated time- and dose-dependent endocytosis [22, 25]. We further demonstrated in the present study that the endocytosis of 5-FU/LDH nanohybrids is an energy-dependent process by incubating cells at 4^{o}C for 4 h after exposure to Red siRNA 546-5-FU/LDH or Red siRNA 546/LDH. The confocal images in Fig. 3C and 3D show that there was no red fluorescence in the cytoplasm and the nucleus, indicating that cellular entry of 5-FU/LDH and LDH-Cl were significantly inhibited at 4^{o}C. Therefore, LDH nanoparticles enter cells through an energy-dependent endocytic mechanism.

Moreover, recent studies on cellular uptake meachanisms and cellular trafficking of LDH particles reveal that LDH cellular uptake undergoes a clathrin-mediated endocytosis pathway in

various cell lines [31, 34]. We reported that LDH has a unique capacity for 'endosmal escape' (similar to the proton sponge effect) and can buffer an endosomal/lysosomal environment (pH 4-5) in virtue of partial dissolution of LDHs, thus allowing LDH to quickly escape from the endosome/lysosome and release loaded drugs/siRNA into the cytoplasm [31]. Therefore, the buffering property of LDH nanoparticles is supposed to promote the delivery of both siRNA and 5-FU into MCF-7 cells, leading to the anticancer efficacy, as presented below.

3.4 Cytotoxicity to cancer cells

Firstly, the cytotoxicity of LDH-Cl nanocarriers to MCF-7 cells in the concentration range of 50 - 200 μg/mL was examined. As shown in Fig. 4, the cell viability was all above 90% following a 3-day incubation, suggesting that LDH nanoparticles do not induce acute cytotoxicity and are well compatible to cancer cells. This is consistent with our previous reports that LDH nanoparticles do not inhibit cell proliferation even at LDH concentrations up to 500 μg/mL in various cell lines [20-22, 25, 33]. Therefore, LDH nanoparticles could be safely used as a drug and gene delivery system.

We then examined the cytotoxicity of 5-FU and 5-FU/LDH to MCF7 cells. As shown in Fig. 5, treatment with 5-FU only decreased cell viability in a dose-dependent manner and ~40% of MCF-7 cells died at 9.6 μg/mL, concurring with previous reports [35, 36]. Compared to free 5-FU, 5-FU/LDH caused considerably more MCF7 cell death and decreased cell viability further by 20-30% at each concentration point in the range of 0.6-9.6 μg/mL, with cancer cell mortality over 60% at 2.4 μg/mL or higher concentrations of 5-FU. The enhancement of 5-FU cytotoxicity to cancer cells through LDH delivery has also been observed by Choy et al [20]. This

enhancement can be attributed to the more efficient cellular uptake of 5-FU mediated by LDH nanoparticles compared to 5-FU only, as reported for the cellular uptake of negatively charged FITC and dsDNA [31].

Treatment with CD-siRNA only did not cause obvious cell death even at 80 nM in the medium (data not shown), mainly because the negative charge of siRNA limits its cellular uptake. When CD-siRNA was loaded with LDH and used to treat cells, ~35% of MCF-7 cells were killed at 40 nM (Fig. 5). The enhanced cytotoxicity can be attributed to the offset of the negative charge of siRNA by positively charged LDH; therefore LDH can effectively deliver siRNA (Fig. 4A) and suppress cell growth [25].

Remarkably, a combination treatment of CD-siRNA and 5-FU, co-delivered by LDH, further decreased cell viability, particularly at the lower 5-FU concentrations (Fig. 5). For example, treatment with CD-siRNA-5-FU/LDH nanocomplexes (1.2 μg/mL of 5-FU and 40 nM of siRNA) caused ~70% cell death, while treatment with either 5-FU/LDH or siRNA/LDH at the same concentration resulted in only 46% or 34% cell death. These data clearly show that a combination treatment with CD-siRNA and 5-FU with LDH nanoparticles significantly suppresses MCF-7 cell growth, probably a result of the synergistic effect of two therapeutics on cancer cells by effectively inducing cell death in complementary pathways [7, 37, 38].

To investigate whether cell death induced by 5-FU and CD siRNA is through early apoptosis, an Annexin V kit was used to analyze the early apoptosis after a 24-hour treatment. As shown in Fig. 6 (right bottom) and listed in Table 2, we did not see an obvious change in the cell population stained with Annexin V. Rather, we saw an increase in the cell population stained

with PI (left top in Fig. 6 and second line in Table 2). This suggests that early apoptosis or membrane damage was not the major pathway for the cell death caused by 5-FU and CD siRNA.

As is well known, the overexpression of the antiapoptotic protein Bcl-2 is one of the major mechanisms by which various cancer cells acquire resistance to apoptosis and thereby resistance to chemotherapeutic agents such as 5-FU. Therefore, western blotting was further conducted to analyze anti-apoptosis protein Bcl-2. As shown in Fig. 7 and listed in Table 2, the combination treatment with CD siRNA-5-FU/LDH nanohybrids significantly decreased the level of Bcl-2, suggesting coordinate mitochondrial damage following treatment [10]. There may be a few possible ways to explain how 5-FU and CD siRNA can lead to Bcl-2 reduction [39]. One explanation relates to thymidine. It is known that 5-FU can interrupt the function of thymidylate synthase that blocks synthesis of the pyrimidine thymidine, which is a nucleoside required for DNA replication [36]. When the cells lack pyrimidine thymidine, the rapidly dividing cancerous cells die via a thymineless death [4]. In mitochondria, the lack of thymidine can also promote apoptosis. A previous study demonstrated that thymidine can attenuate adenosine-induced apoptosis by modulating the earliest stage of the mitochondrial apoptotic pathway [40], suggesting that certain levels of thymidine will protect mitochondria from apoptosis. Further studies may be needed to prove this. So far, the mechanism of CD siRNA causing cell death is not clear, and therefore no explanation can be given for its related Bcl-2 reduction.

3.5 Applicability to other cell lines

We have finally confirmed that our co-delivery strategy using LDH nanoparticles for effective cancer treatment can be applied to other cancer cell lines, such as U2OS and HCT-116. As

shown in Fig. S3A and S3B, a combination treatment of U2OS and HCT-116 cells with CD-siRNA and 5-FU delivered by LDH resulted in significant suppression of cell growth compared to single treatment with either CD-siRNA/LDH or 5-FU/LDH alone. These results indicated that a combination treatment with CD-siRNA and 5-FU produced a synergistic inhibition effect on the cell growth of various cancers.

4. Conclusions

In summary, we have successfully developed a combined strategy that applies the LDH delivery system to simultaneously deliver CD-siRNA and chemotherapeutic drug 5-FU to cancer cells for effective cancer treatment. Our data clearly indicate that combination treatment with siRNA and 5-FU co-delivered by LDHs can lead to significantly higher cytotoxicity to three cancer cell lines (MCF-7, U2OS and HCT-116) compared to the single treatment with either CD siRNA or 5-FU. Therefore, co-delivery of siRNAs and anticancer drugs by LDHs has great potential as a novel approach for effective cancer treatment.

Acknowledgements

The authors acknowledge the facilities, and the scientific and technical assistance of the Australian Microscopy & Microanalysis Research Facility at the Centre for Microscopy and Microanalysis and Australian National Fabrication Facility (Qld Node), The University of Queensland. The study was supported by ARC Future Fellowship (FT120100813), ARC DP grant (DP120104792), the University of Queensland Postdoctoral Fellowship and UQ early-career-research grant.

References

[1] Peer D, Karp JM, Hong S, Farokhzad OC, Margalit R, Langer R. Nanocarriers as an emerging platform for cancer therapy. Nat Nanotechnol 2007;2:751-760.

[2] Gillet JP, Gottesman M. Mechanisms of multidrug resistance in cancer. In: Zhou J, editor. Multi-drug resistance in cancer. Humana Press, 2010. p. 47-76.

[3] Saad M, Garbuzenko OB, Minko T. Co-delivery of siRNA and an anticancer drug for treatment of multidrug-resistant cancer. Nanomedicine 2008;3:761-776.

[4] Longley DB, Harkin DP, Johnston PG. 5-Fluorouracil: mechanisms of action and clinical strategies. Nat Rev Cancer 2003;3:330-338.

[5] Chang RS, Suh MS, Kim S, Shim G, Lee S, Han SS, et al. Cationic drug-derived nanoparticles for multifunctional delivery of anticancer siRNA. Biomaterials 2011;32:9785-9795.

[6] Tan SJ, Kiatwuthinon P, Roh YH, Kahn JS, Luo D. Engineering nanocarriers for siRNA delivery. Small 2011;7:841-856.

[7] Khan M, Ong ZY, Wiradharma N, Attia ABE, Yang YY. Advanced materials for co-delivery of drugs and genes in cancer therapy. Adv Healthc Mater 2012;1:373-392.

[8] Fan H, Hu QD, Xu FJ, Liang WQ, Tang GP, Yang WT. In vivo treatment of tumors using host-guest conjugated nanoparticles functionalized with doxorubicin and therapeutic gene pTRAIL. Biomaterials 2012;33:1428-436.

[9] Hu CMJ, Aryal S, Zhang L. Nanoparticle-assisted combination therapies for effective cancer treatment. Ther Deliv 2010;1:323-334.

This is a post-print version of the following article: Li, Li, Gu, Wenyi, Chen, Jiezhong, Chen, Weiyu and Xu, Zhi P. (2014) Co-delivery of siRNAs and anti-cancer drugs using layered double hydroxide nanoparticles. *Biomaterials*, *35* 10: 3331-3339.

[10] Nakamura K, Abu Lila AS, Matsunaga M, Doi Y, Ishida T, Kiwada H. A double-modulation strategy in cancer treatment with a chemotherapeutic agent and siRNA. Mol Ther 2011;19:2040-2047.

[11] Chen AM, Zhang M, Wei D, Stueber D, Taratula O, Minko T, et al. Co-delivery of doxorubicin and Bcl-2 siRNA by mesoporous silica nanoparticles enhances the efficacy of chemotherapy in multidrug-resistant cancer cells. Small 2009;5:2673-2677.

[12] Wang H, Zhao Y, Wu Y, Hu Yl, Nan K, Nie G, et al. Enhanced anti-tumor efficacy by co-delivery of doxorubicin and paclitaxel with amphiphilic methoxy PEG-PLGA copolymer nanoparticles. Biomaterials 2011;32:8281-8290.

[13] Cheng D, Cao N, Chen J, Yu X, Shuai X. Multifunctional nanocarrier mediated co-delivery of doxorubicin and siRNA for synergistic enhancement of glioma apoptosis in rat. Biomaterials 2012;33:1170-1179.

[14] Xu ZP, Brateman PS, Yarberry F, Layer double hydroxides In: SM Auerbach, KA Carrado and PK Dutta (eds) Handbook of layered materials. Marcel Dekker, Inc New York 2004:373.

[15] Ladewig K, Xu ZP, Lu GQ. Layered double hydroxide nanoparticles in gene and drug delivery. Expert Opin Drug Deliv 2009;6:907-922.

[16] Xu ZP, Stevenson G, Lu CQ, Lu GQ, Bartlett PF, Gray P. Stable suspension of layered double hydroxide nanoparticles in aqueous solution. J Am Chem Soc 2006;128:36-37.

[17] Choi SJ, Choi GE, Oh JM, Oh YJ, Park MC, Choy JH. Anticancer drug encapsulated in inorganic lattice can overcome drug resistance. J Mater Chem 2010;20:9463-9469.

[18] Chakraborty M, Dasgupta S, Sengupta S, Chakraborty J, Ghosh S, Ghosh J, et al. A facile synthetic strategy for Mg-Al layered double hydroxide material as nanocarrier for methotrexate. Ceram Int 2012;38:941-949.

[19] Pan DK, Zhang H, Fan T, Chen JG, Duan X. Nearly monodispersed core-shell structural Fe_3O_4@DFUR-LDH submicro particles for magnetically controlled drug delivery and release. Chem Commun 2011;47:908-910.

[20] Choi SJ, Oh JM, Choy JH. Anticancer drug-layered hydroxide nanohybrids as potent cancer chemotherapy agents. J Phys Chem Solids 2008;69:1528-1532.

[21] Ladewig K, Niebert M, Xu ZP, Gray PP, Lu GQM. Efficient siRNA delivery to mammalian cells using layered double hydroxide nanoparticles. Biomaterials 2010;31:1821-1829.

[22] Wong Y, Markham K, Xu ZP, Chen M, Lu GQ, Bartlett PF, et al. Efficient delivery of siRNA to cortical neurons using layered double hydroxide nanoparticles. Biomaterials 2010;31:8770-8779.

[23] Choy JH, Jung JS, Oh JM, Park M, Jeong J, Kang YK, et al. Layered double hydroxide as an efficient drug reservoir for folate derivatives. Biomaterials 2004;25:3059-3064.

[24] Oh JM, Park M, Kim ST, Jung JY, Kang YG, Choy JH. Efficient delivery of anticancer drug MTX through MTX-LDH nanohybrid system. J Phys Chem Solids 2006;67:1024-1027.

[25] Chen M, Cooper HM, Zhou JZ, Bartlett PF, Xu ZP. Reduction in the size of layered double hydroxide nanoparticles enhances the efficiency of siRNA delivery. J Colloid Interface Sci 2013;390:275-281.

[26] Xu ZP, Stevenson G, Lu CQ, Lu GQ. Dispersion and size control of layered double hydroxide nanoparticles in aqueous solutions. J Phys Chem B 2006;110:16923-16929.

[27] Liu CX, Hou WG, Li LF, Li Y, Liu SJ. Synthesis and characterization of 5-fluorocytosine intercalated Zn-Al layered double hydroxide. J Solid State Chem 2008;181:1792-1797.

[28] Wang Z, Wang E, Gao L, Xu L. Synthesis and properties of Mg2Al layered double hydroxides containing 5-fluorouracil. J Solid State Chem 2005;178:736-741.

[29] Chen CP, Yee LK, Gong H, Zhang Y, Xu R. A facile synthesis of strong near infrared fluorescent layered double hydroxide nanovehicles with an anticancer drug for tumor optical imaging and therapy. Nanoscale 2013;5:4314-4320.

[30] Xu ZP, Gu Z, Cheng XX, Rasoul F, Whittaker AK, Lu GQM. Controlled release of ketorolac through nanocomposite films of hydrogel and LDH nanoparticles. J Nanopart Res 2011;13:1253-1264.

[31] Xu ZP, Niebert M, Porazik K, Walker TL, Cooper HM, Middelberg APJ, et al. Subcellular compartment targeting of layered double hydroxide nanoparticles. J Control Release 2008;130:86-94.

[32] Yassin AE, Anwer MK, Mowafy HA, El-Bagory IM, Bayomi MA, Alsarra IA. Optimization of 5-flurouracil solid-lipid nanoparticles: a preliminary study to treat colon cancer. Int J Med Sci 2010;7:398-408.

[33] Ladewig K, Niebert M, Xu ZP, Gray PP, Lu GQ. Controlled preparation of layered double hydroxide nanoparticles and their application as gene delivery vehicles. Appl Clay Sci 2010;48:280-289.

[34] Oh JM, Choi SJ, Kim ST, Choy JH. Cellular uptake mechanism of an inorganic nanovehicle and its drug conjugates: enhanced efficacy due to clathrin-mediated endocytosis. Bioconjug Chem 2006;17:1411-1417.

[35] Chumakova OV, Liopo AV, Evers BM, Esenaliev RO. Effect of 5-fluorouracil, optison and ultrasound on MCF-7 cell viability. Ultrasound Med and Bio 2006;32:751-8.

[36] Chow L, Loo W. The differential effects of cyclophosphamide, epirubicin and 5-fluorouracil on apoptotic marker (CPP-32), proapoptotic protein (p21WAF-1) and anti-apoptotic protein (bcl-2) in breast cancer cells. Breast Cancer Res Treat 2003;80:239 -244.

[37] Xiong XB, Lavasanifar A. Traceable multifunctional micellar nanocarriers for cancer-targeted co-delivery of MDR-1 siRNA and doxorubicin. ACS Nano 2011;5:5202-5013.

[38] Hu CMJ, Zhang L. Nanoparticle-based combination therapy toward overcoming drug resistance in cancer. Biochem Pharmacol 2012;83:1104-1111.

[39] Elmore S. Apoptosis: a review of programmed cell death. Toxicol Pathol 2007;35:495-516.

[40] Kang CM, Suh Y, Jang IS, Park SC. Thymidine-dependent attenuation of the mitochondrial apoptotic pathway in adenosine-induced apoptosis of HL-60 cells. J Cancer Res Clin Oncol 2001;127:570-576.

This is a post-print version of the following article: Li, Li, Gu, Wenyi, Chen, Jiezhong, Chen, Weiyu and Xu, Zhi P. (2014) Co-delivery of siRNAs and anti-cancer drugs using layered double hydroxide nanoparticles. *Biomaterials*, *35* 10: 3331-3339.

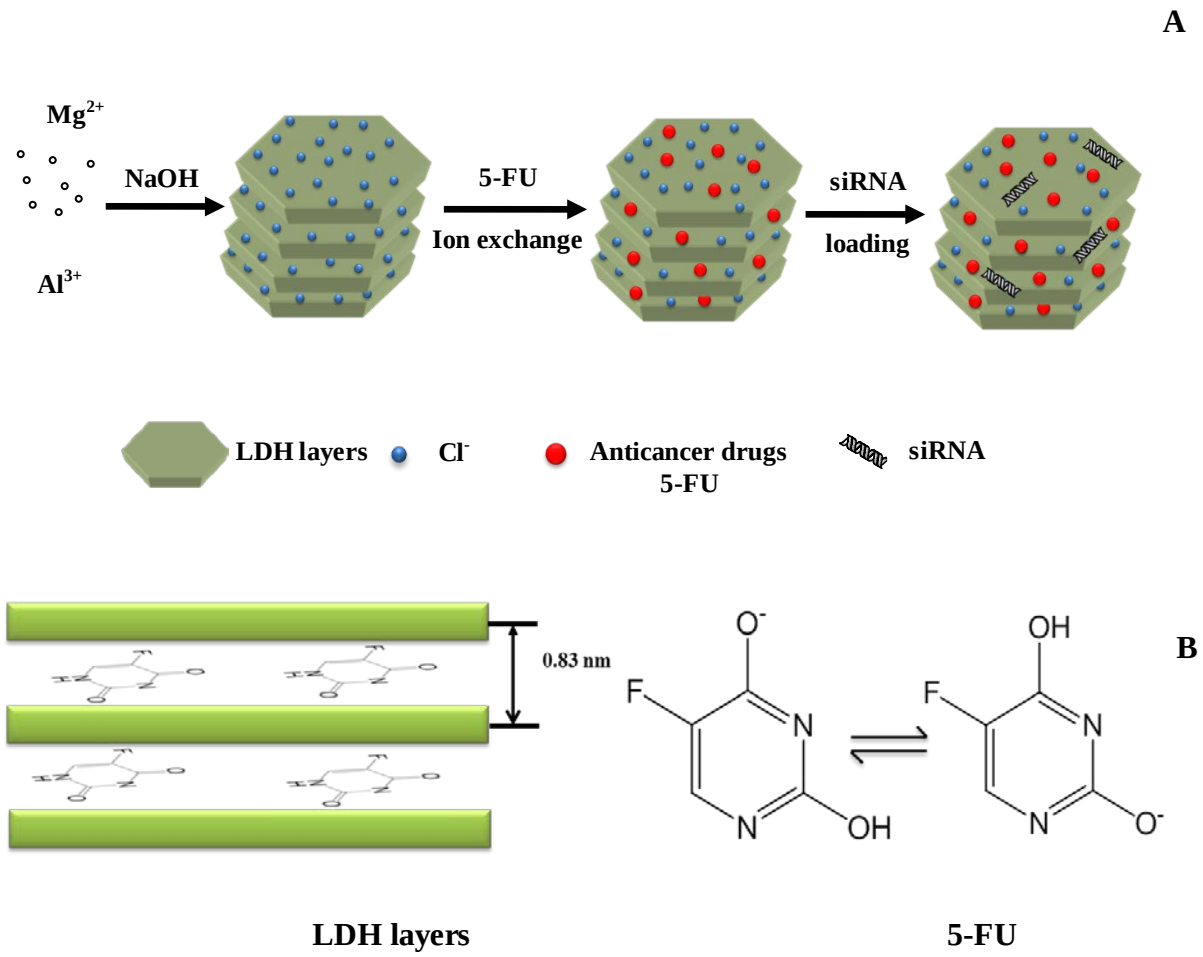

Scheme 1 Schematic diagram of the LDH co-delivery system to co-load 5-FU and siRNA (A) and schematic illustration of the horizontal laying of 5-FU in the interlayer (B)

This is a post-print version of the following article: Li, Li, Gu, Wenyi, Chen, Jiezhong, Chen, Weiyu and Xu, Zhi P. (2014) Co-delivery of siRNAs and anti-cancer drugs using layered double hydroxide nanoparticles. *Biomaterials*, *35* 10: 3331-3339.